J. Biochem. 132, 93–102 (2002)

Ca^{2+}- and S1-Induced Movement of Troponin T on Reconstituted Skeletal Muscle Thin Filaments Observed by Fluorescence Energy Transfer Spectroscopy[1]

Chieko Kimura,[*] Kayo Maeda,[†] Yuichiro Maéda,[†] and Masao Miki[*,2]

[*]*Department of Applied Chemistry and Biotechnology, Fukui University, 3-9-1 Bunkyo, Fukui 910-8507; and* [†]*Riken Harima Institute at Spring8, Mikazuki-cho, Sayo, Hyogo, 679-5143*

Received April 12, 2002; accepted May 4, 2002

Troponin T (TnT) is an essential component of troponin (Tn) for the Ca^{2+}-regulation of vertebrate striated muscle contraction. TnT consists of an extended NH_2-terminal domain that interacts with tropomyosin (Tm) and a globular COOH-terminal domain that interacts with Tm, troponin I (TnI), and troponin C (TnC). We have generated two mutants of a rabbit skeletal β-TnT 25-kDa fragment (59–266) that have a unique cysteine at position 60 (N-terminal region) or 250 (C-terminal region). To understand the spatial rearrangement of TnT on the thin filament in response to Ca^{2+} binding to TnC, we measured distances from Cys-60 and Cys-250 of TnT to Gln-41 and Cys-374 of F-actin on the reconstituted thin filament by using fluorescence resonance energy transfer (FRET). The distances from Cys-60 and Cys-250 of TnT to Gln-41 of F-actin were 39.5 and 30.0 Å, respectively in the absence of Ca^{2+}, and increased by 2.6 and 5.8 Å, respectively upon binding of Ca^{2+} to TnC. The rigor binding of myosin subfragment 1 (S1) further increased these distances by 4 and 5 Å respectively, when the thin filaments were fully decorated with S1. This indicates that not only the C-terminal but also the N-terminal region of TnT showed the Ca^{2+}- and S1-induced movement, and the C-terminal region moved more than N-terminal region. In the absence of Ca^{2+}, the rigor S1 binding also increased the distances to the same extent as the presence of Ca^{2+} when the thin filaments were fully decorated with S1. The addition of ATP completely reversed the changes in FRET induced by rigor S1 binding both in the presence and absence of Ca^{2+}. However, plots of the extent of S1-incuced conformational change vs. molar ratio of S1 to actin showed hyperbolic curve in the presence of Ca^{2+} but sigmoidal curve in the absence of Ca^{2+}. FRET measurement of the distances from Cys-60 and Cys-250 of TnT to Cys-374 of actin showed almost the same results as the case of Gln-41 of actin. The present FRET measurements demonstrated that not only TnI but also TnT change their positions on the thin filament corresponding to three states of thin filaments (relaxed, Ca^{2+}-induced or closed, and S1-induced or open states).

Key words: FRET, regulation, troponin T, thin filament, three states of thin filament.

In striated muscle, the interaction between actin and myosin is regulated by tropomyosin (Tm) and troponin (Tn) on the actin filament in response to changes of intracellular Ca^{2+} concentration (*1*). Tn consists of three different subunits, TnC, TnI, and TnT. The globular part of troponin, composed of TnC and TnI, binds to tropomyosin near Cys-190 (residues 150–180), and the elongated part, composed of TnT, covers over an extensive region of the COOH-terminal half of tropomyosin. TnI alone inhibits the actomyosin ATPase, and the inhibition is removed on adding TnC irrespective of Ca^{2+} concentration. TnT is required for full Ca^{2+}-regulation of the ATPase activity of a reconstituted system. Troponin T is split into two subfragments, TnT1 (1–158) and TnT2 (159–259) by mild treatment with chymotrypsin (*2*). The amino-terminal region TnT1 binds to Tm in a Ca^{2+}-independent manner, while the carboxyl-terminal region TnT2 binds to TnI, TnC and also Tm. In particuar, the C-terminal 17 residues of TnT2 contain the Tm-binding site that is critical for the Ca^{2+}-sensitizing activity of TnT (*3*). A 26-kDa fragment of TnT that lacks the N-terminal 52 amino acid residues was found to have the same properties

[1] This study was performed with Special Coordination Funds of the Ministry of Education, Culture, Sports, Science and Technology, the Japanese Government.

[2] To whom correspondence should be addressed. Tel: +81-776-27-8786, Fax: +81-776-27-8747, E-mail: masao@acbio.fukui-u.ac.jp

Abbreviations: 3D-EM, three-dimensional image reconstruction of electron micrographs; DABMI, 4-dimethyl-aminophenylazophenyl 4′-maleimide; FLC, fluorescein cadaverine; FRET, fluorescence resonance energy transfer; IAEDANS, 5-(2-iodoacetylaminoethyl)aminonaphthalene 1-sulfonic acid; S1, myosin subfragment 1; Tm, tropomyosin; TnT 25k, a mutant rabbit skeletal β-troponin T 25-kDa fragment which lacks the N-terminal region 1–58; AEDANS-60-TnT, TnT 25k (E60C) in which the second (60th in full-length TnT) glutamate was replaced with cysteine and labeled with IAEDANS; AEDANS-250-TnT, TnT 25k (S250C) in which 192nd (250th in full-length TnT) serine was replaced with cysteine and labeled with IAEDANS; Tn, troponin; AEDANS-60-Tn, the reconstituted troponin complex using AEDANS-60-TnT; AEDANS-250-Tn, the reconstituted Tn using AEDANS-250-TnT.

as the intact TnT with regard to both the Ca^{2+}-regulating action and tropomyosin binding (*4*). A β-type TnT 25 kDa fragment of rabbit skeletal muscle that lacks the entire N-terminal variable region and contains near the carboxyl-terminus a segment of 14 residues that is changed from the α-type to the β-type sequence, was expressed in *Escherichia coli*. This 25-kDa fragment (residues: 59–266) is functionally identical to the native α-TnT and is soluble at low ionic strength, unlike the native α-TnT (*5*).

Numerous studies have characterized the interaction between the thin filament proteins to deduce how the Ca^{2+}-triggering signal is propagated from TnC to the rest of the thin filament [for a review, see Gordon *et al.* (*6*)]. Recent biochemical studies suggest that there may be three states of the thin filament (blocked, closed, and open) (*7–9*). The equilibrium between blocked and closed states is Ca^{2+}-sensitive, and strong S1 binding induces the fully activated open state. X-ray diffraction data of skinned fibers or oriented filaments and 3D-EM data of isolated thin filaments have been interpreted to indicate three positions of Tm corresponding to the three-state model. This interpretation supports the steric blocking theory in which Tm blocks the myosin binding site by changing the positions on an actin filament (*10, 11*). However, the Ca^{2+}-induced conformational change of the thin filament cannot clearly be assigned as a Tm movement from these data, since the contributions of Tn and/or actin conformational changes are neglected in these analyses. Recent 3D-EM demonstrated that the main body of Tn moves with Tm towards the outer domain of the actin filament during inhibition (*12, 13*). On the other hand, fluorescence resonance energy transfer (FRET) has been extensively used for studying the spatial relationships between residues on muscle proteins (*14, 15*). This method is especially valuable for detecting small conformational changes, since the transfer efficiency is a function of the inverse of the sixth power of the distance between probes. In this method, fluorescence donor and acceptor molecules are specifically labeled so that the assignment of the conformational change is direct. Several attempts have been made to detect conformational changes of Tm and Tn on the reconstituted thin filament. With Ca^{2+} binding to TnC, the distances between Cys-133 of TnI and Cys-374, Gln-41 or the nucleotide-binding site of actin increased by 10–15 Å (*16–21*). The distance was increased further by ~7 Å by rigor S1 binding (*20, 21*). FRET measurements clearly showed that the inhibitory and C-terminal regions of TnI change their positions on actin, corresponding to three states of the thin filament (locked, closed, and open). However, the transfer efficiency between probes attached to Tm (at position 87 or 190) and actin (at position 41, 61, 374, or the nucleotide-binding site) was little sensitive to Ca^{2+}- or S1-binding (*16, 22–24*).

Among Tn subunits, TnT has not been used much for FRET measurements, partly due to the relatively low solubility of this protein and perhaps also because of the lack of a cysteine residue for fluorescence labeling in all known vertebrate isoforms other than bovine cardiac TnT. In the present study, we have generated single-thiol mutants of a rabbit skeletal β-type TnT 25-kDa fragment in which a single cysteine residue was introduced at position 60 (numbering is on the full-length TnT) in the N-terminal region or 250 in the C-terminal region. Then FRET between these points of TnT and Cys-374 or Gln-41 of actin on reconstituted thin filaments was measured in the presence or absence of Ca^{2+} ion or S1.

MATERIALS AND METHODS

Reagents—Phalloidin from *Amantina phalloides* was purchased from Boehringer Mannheim Biochemica. IAEDANS, DABMI, and FLC were purchased from Molecular Probes. BCA Protein assay reagent was from Pierce Chemicals. All other chemicals were analytical grade.

Protein Preparations—Actin, S1, and Tn were prepared from rabbit skeletal muscle as reported previously (*16*). α-Tm was extracted from rabbit hearts as previously reported (*16*). Microbial transglutaminase was a generous gift from Food Research and Development Laboratories, Ajinomoto.

Single-cysteine TnT25k mutants were constructed using a recombinant 25-kDa fragment of TnT, the sequence of which was based on the rabbit fast skeletal muscle β-TnT and lacks 58 amino acid residues at the N-terminus. The numbering of the amino acid sequence in the mutants is the same as in the full-length TnT, so that it begins with 59 and ends at 266. To prepare the mutant TnT25k (E60C) and TnT25k (S250C), we started with a cDNA for a full-length β-TnT (*25*). To construct TnT25k (S250C), mutagenesis was carried out on a pUC119 template using standard protocols of the Sculptor *in vitro* mutagenesis system (Amersham). The oligonucleotide designed as an anti-sense sequence to mutate sense single-stranded DNA was as follows (the mutant codon is underlined): TnT-Ser250Cys, TT CTTGCAGTGCTTC. DNA sequencing screened out clones containing the designed mutations. To construct the expression plasmid pTrc-TnT25k (S250C), the *Acc*I and *Eco*RI fragment from the resultant plasmid was inserted into the plasmid pTrc99C between the *Nco*I and *Eco*RI sites, together with a pair of 14 bp oligonucleotides which fill the gap between the *Nco*I and *Acc*I sites (*5*). To construct TnT25k (E60C), the *Acc*I–*Eco*RI fragment containing the TnT25k coding sequence was inserted into the *Nco*I and *Eco*RI sites of pTrc99C together with a pair of oligonucleotides. The oligonucleotides, which fill the gap between the *Nco*I and *Acc*I sites, were designed to replace Glu-60 with cysteine as follows (the mutant codon is underlined): Glu-60 → Cys, sense: CATGGGTTGTAAAGT; antisense: CTACTTTACAACC. Both mutants in the expression vector were confirmed by DNA sequencing.

Expression and purification of single cysteine TnT25k mutants was carried out as follows. TnT25k (E60C) and TnT25k (S250C) were expressed in AD202 (*26*): 50 ml of the bacterial cells with TnT mutant–expression plasmids were grown overnight at 37°C in LB medium supplemented with 50 μg/ml ampicillin, which was then used to inoculate 1 liter of the same medium. The main culture was shaken at 300 rpm and 37°C for about 1 h until A_{600} reached between 0.7 and 0.8. The addition of IPTG to a final concentration of 0.1 mM started induction of protein expression, and the culture was continued for about 16 h under the same conditions. The cells were harvested by centrifugation at 6,000 ×*g* for 10 min, and washed once with 50 mM Tris-HCl (pH 8.0), 1 mM EDTA. Expressed single cysteine TnT25k mutants went into the insoluble fraction. The cells were frozen, thawed and resuspended in 50 mM Tris-HCl (pH 8.0), 8% sucrose, 5% Triton X-100, and 50 mM EDTA (STET). Lysozyme was added to a concentration of 0.2 mg/

ml and the suspension was incubated at 4°C for 1 h. The mixture was sonicated 3 times each for 5 min. Pellets were collected by centrifugation at 10,000 ×*g* for 30 min and resuspended in STET. The sonication procedure was repeated twice in STET and then once more in 50 mM Tris-HCl (pH 8.0), 1 mM EDTA. The pellets were resuspended in 6 M urea, 50 mM Tris-HCl (pH 8.0), 1 mM EDTA, and 1 mM NaN_3 (solution A) containing inhibitor cocktail (Roche Diagnostics, one tablet per 50 ml of solution), and the suspension was sonicated again. Solubilized TnT25k mutants were obtained in the supernatant after centrifugation at 10,000 ×*g* for 30 min. The supernatant was applied to a Q-sepharose fast flow column (Pharmacia LKB Biotechnology, 2.5 × 10 cm) equilibrated with solution A. The flow-through fraction was then applied to a CM-Toyopearl 650 M column (Toso, 2.5 × 10 cm) equilibrated with solution A. TnT25k mutants were eluted with a 0.5 M NaCl step. The fraction containing TnT25k mutants were dialyzed against 25 mM phosphate buffer (pH 7.0) and 0.5 M KCl, then applied to a Celulofine column (Seikagaku industry, 2.5 × 5 cm) equilibrated with the same buffer. The TnT25k mutants were eluted from the column with 0.25 M phosphate buffer (pH 7.0). Protein concentrations were determined by use of absorption coefficients of A_{290} = 0.63 $(mg/ml)^{-1}$ cm^{-1} for G–actin, and A_{280} = 0.75 $(mg/ml)^{-1}$ cm^{-1} for S1, 0.31 $(mg/ml)^{-1}$ cm^{-1} for Tm, 0.45 $(mg/ml)^{-1}$ cm^{-1} for Tn and 0.67 $(mg/ml)^{-1}$ cm^{-1} for TnT25k. The concentrations of labeled proteins were measured with the BCA protein assay reagent with the respective unlabeled proteins as standards. Relative molecular masses of 42,000 for actin, 115,000 for S1, 66,000 for Tm, 69,000 for Tn, 25,000 for TnT 25K, and 38,000 for transglutaminase were used.

Labeling of Proteins—Actin was labeled at Glu-41 with FLC or at Cys-374 with DABMI as described previously by (*19*). TnT25k mutants were incubated with a 10-fold molar excess of IAEDANS in 0.5 M KCl and 20 mM phosphate buffer (pH 7.0) for 3 h at 25°C. The reaction was terminated by the addition of 1.0 mM DTT, and the sample solution was dialyzed against 5 mM Tris-HCl (pH 8.0) and 0.4 M KCl exhaustively to remove free IAEDANS.

Reconstitution of Ternary Tn Complexes with AEDANS-Labeled TnT25k Mutants—Tn subunits including TnT25k mutants were combined in a solution containing 6 M urea, 0.4 M KCl, 1 mM $CaCl_2$, 1 mM dithiothreitol and 20 mM Tris-HCl (pH 8.0). TnT25k mutants, TnC and TnI were mixed in a molar ratio 1:1:1.2. The mixture was then dialyzed consecutively against KCl solutions of 1 M, 0.5 M, 0.3 M, 0.1 M, and 30 mM, each containing 1 mM $CaCl_2$, 10 mM β-mercaptoethanol and 20 mM Tris-HCl (pH 8.0). After dialysis, the protein solution was clarified by centrifugation and applied to a Hitrap-Q column (Pharmacia) equilibrated with 30 mM KCl, 1 mM $CaCl_2$, and 20 mM Tris-HCl (pH 8.0). The ternary complex was eluted with a linear gradient of 30 mM–0.3 M KCl in the same solution. Fractions containing pure complex were identified by SDS gel electrophoresis. The purified Tn complex was dialyzed against 5 mM Tris-HCl (pH 8.0) and 0.1 M KCl.

Spectroscopic Measurements—Absorption was measured with a Hitachi U2000 spectrophotometer. Steady-state fluorescence was measured with a Perkin Elmer LS50B fluorometer. The temperature was maintained at 20°C. The absorption coefficients of 24,800 M^{-1} cm^{-1} at 460 nm for DABMI (*27*), 75,500 M^{-1} cm^{-1} at 493 nm for FLC (*28*), and 6,100 M^{-1} cm^{-1} at 334 nm for IAEDANS (*29*) were used for the determination of labeling ratios. The typical labeling ratios were 0.96 for DAB-F-actin, 1.0 for FLC-F-actin, 0.75 for AEDANS-250-Tn, and 0.74 for AEDANS-60-Tn.

Fluorescence Resonance Energy Transfer—The efficiency E of resonance energy transfer between probes was determined by measuring the fluorescence intensity of the donor in the presence (F_{DA}) and absence (F_{D0}) of the acceptor as given by

$$E = 1 - F_{DA}/F_{D0} \quad (1)$$

The efficiency is related to the distance (R) between donor and acceptor, and Förster's critical distance (R_0) at which the transfer efficiency is equal to 50% by

$$E = R^6/(R^6+R_0^6) \quad (2)$$

R_0 can be obtained (in nm) with

$$R_0^6 = (8.79 \times 10^{-11})\, n^{-4}\kappa^2 Q_0 J \quad (3)$$

where n is the refractive index of the medium taken as 1.4, κ^2 is the orientation factor, Q_0 is the quantum yield of the donor in the absence of the acceptor, and J is the spectral overlap integral between the donor emission F_D (λ) and acceptor absorption $\varepsilon_A(\lambda)$ spectra defined by

$$J = \int F_D(\lambda)\, \varepsilon_A(\lambda)\lambda^4 d\lambda / \int F_D(\lambda)\, d\lambda \quad (4)$$

The quantum yield was determined by a comparative method using quinine sulfate in 1 M H_2SO_4 as the standard, which has an absolute quantum yield of 0.70 (*30*). κ^2 was taken as 2/3 for calculation of distances. The decrease of the fluorescence intensity due to inner filter effects was corrected with

$$F_{corr} = F_{obs} \times 10^{(Aex+Aem)/2} \quad (5)$$

where A_{ex} and A_{em} are absorption of the sample at the excitation and emission wavelengths, respectively.

Other Methods—Mg-ATPase activity was measured by the method of Tausky and Shorr (*31*). Measurements were performed at 25°C in 10 mM KCl, 5 mM $MgCl_2$, 2 mM ATP, 20 mM Tris-HCl (pH 7.6), 1 mM DTT and 50 μM $CaCl_2$ for the $+Ca^{2+}$ state or 1 mM EGTA for the $-Ca^{2+}$ state. Protein concentrations were 4 μM F-actin, 0.57 μM Tm, 0.67 μM Tn and 1 μM S1.

DNA sequencing was performed using the ABI PRISM 377 DNA Sequencing System (ABI PRISM BigDye Terminator Cycle Sequencing Ready Reaction Kit; Applied Biosystems). We used -21M13 universal primer or appropriate specific primers synthesized based on Ptrc99C sequences.

RESULTS

The AEDANS moiety bound to Cys-60 or Cys-250 of mutant 25-kDa fragments of β-TnT was used as the energy donor, while FLC or DABMI attached to Gln-41 or Cys-374 of actin, respectively, was used as the energy transfer acceptor. Cys-60 is located at the 2nd residue from the N-terminus and Cys-250 at the 17th residue from the C-terminus of the 25-kDa fragment of TnT. The regulatory activity of Tn complexes reconstituted with the AEDANS-labeled TnT25k mutants was tested. The MgATPase activities of the reconstituted system composed of F-actin, S1, Tm and the mutant Tn complexes were measured in the presence and absence of Ca^{2+}. The mutant Tn complexes

inhibited acto-S1-MgATPase activity in the absence of Ca^{2+}, and the inhibition was released by the addition of Ca^{2+} as efficiently as that of the wild-type Tn complex. ATPase measurements indicate that neither the mutation nor the labeling of AEDANS affected the regulatory activity of TnT.

FRET between Cys-60 or Cys-250 of TnT and Gln-41 or Cys-374 of F-Actin on Reconstituted Thin Filaments in the Presence and Absence of Ca^{2+}—The absorption spectrum of FLC bound to actin overlaps well with the fluorescence emission spectrum of AEDANS bound to TnT (Cys-60 and 250). The overlap integral, J, was calculated to be 16.6×10^{14} M^{-1} cm^{-1} nm^4 for the AEDANS-60-Tn/FLC-F-actin pair and 17.4×10^{14} M^{-1} cm^{-1} nm^4 for the AEDANS-250-Tn/FLC-F-actin pair. The quantum yields of AEDANS-60-Tn were 0.26 and 0.30 in the presence and absence of Ca^{2+}, respectively, and those of AEDANS-250-Tn were 0.34 and 0.37 in the presence and absence of Ca^{2+}, respectively. By taking of $n = 1.4$ and $\kappa^2 = 2/3$, the Förster's critical distance, R_0, for the AEDANS-60-Tn/FLC-F-actin pair was determined to be 43.3 and 44.3 Å in the presence and absence of Ca^{2+}, respectively. R_0 for the AEDANS-250-Tn/FLC-F-actin pair was determined to be 45.6 and 46.3 Å in the presence and absence of Ca^{2+}, respectively.

Figure 1 shows the fluorescence spectra of AEDANS-250-Tn on the reconstituted thin filaments in the presence (curves 2 and 5) and absence (curves 1 and 4) of an acceptor (FLC bound to F-actin). The solvent conditions were 30 mM KCl, 20 mM Tris-HCl (pH 7.6), 2 mM $MgCl_2$, 0.1 mM ATP, 1 mM NaN_3 (buffer F), and 50 μM $CaCl_2$ for the $+Ca^{2+}$ state (curves 1 and 2) or 1 mM EGTA for the $-Ca^{2+}$ state (curves 4 and 5) at 20°C. The donor fluorescence was significantly quenched in the presence of the acceptor at wavelengths shorter than 480 nm. This can be attributed mainly to resonance energy transfer from AEDANS-Tn to FLC-F-actin. Removal of free Ca^{2+} ions by the addition of 1 mM EGTA increased the donor fluorescence intensity in the absence of the acceptor but, on the contrary, decreased it significantly in the presence of the acceptor. The transfer efficiency on reconstituted thin filaments was greater in the absence than that in the presence of Ca^{2+}. The fluorescence spectra of AEDANS-60-Tn on the reconstituted thin filaments were also measured in the presence and absence of the acceptor (FLC bound to F-actin) under the same solvent conditions as AEDANS-250-Tn, and almost the same results were observed. Compared with AEDANS-60-Tn, the fluorescence intensity of AEDANS-250-Tn was substantially quenched by FLC-F-actin in the presence of Ca^{2+}, and the extent of quenching was greatly increased by removal of Ca^{2+}. The results indicate that the C-terminal region of TnT is located closer to Gln-41 of F-actin than the N-terminal region, and that the Ca^{2+}-induced distance change of the C-terminal region was larger than that of the N-terminal region of TnT.

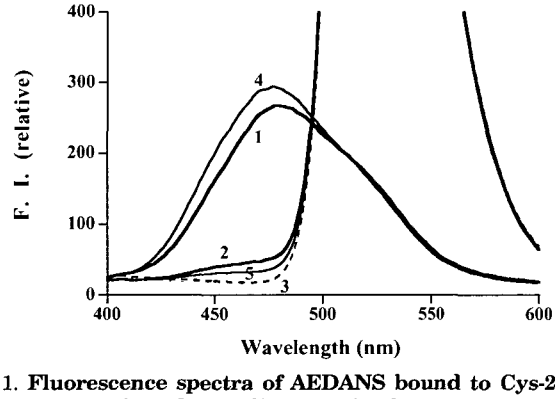

Fig. 1. **Fluorescence spectra of AEDANS bound to Cys-250 of TnT on reconstituted thin filaments in the presence and absence of an acceptor (FLC bound to Gln-41 of actin).** (1) F-actin/Tm/AEDANS-Tn/$+Ca^{2+}$, (2) FLC-F-actin/Tm/AEDANS-Tn/$+Ca^{2+}$, (3) FLC-F-actin/Tm/Tn/$\pm Ca^{2+}$, (4) F-actin/Tm/AEDANS-Tn/$-Ca^{2+}$, (5) FLC-F-actin/Tm/AEDANS-Tn/$-Ca^{2+}$. Spectra were measured at 20°C in 30 mM KCl, 2 mM $MgCl_2$, 20 mM Tris-HCl (pH7.6), 1 mM NaN_3 (buffer F), and 50 μM $CaCl_2$ for the $+Ca^{2+}$ state or 1 mM EGTA for the $-Ca^{2+}$ state. The concentrations of actin, Tm and Tn were 0.2, 0.044, and 0.042 mg/ml, respectively. Excitation was at 340 nm. The fluorescence spectra of curves 2, 3, and 5 at wavelengths longer than 480 nm, which are derived mainly from FLC with an emission peak at 520 nm, are omitted from the figure.

FRET between DABMI attached to Cys-374 on F-actin and AEDANS-60-Tn or AEDANS-250-Tn was measured. The overlap integral, J, was calculated to be 6.52×10^{14} M^{-1} cm^{-1} nm^4 for the AEDANS-60-Tn/DAB-F-actin pair and 6.64×10^{14} M^{-1} cm^{-1} nm^4 for the AEDANS-250-Tn/DAB-F-actin pair. The Förster's critical distance, R_0, of AEDANS-60-Tn/DAB-F-actin pair was determined to be 37.1 and 37.9 Å in the presence and absence of Ca^{2+}, respectively. R_0 of the AEDANS-250-Tn/DAB-F-actin pair was determined to be 38.9 and 39.4 Å in the presence and absence of Ca^{2+}, respectively. Figure 2 shows the fluorescence spectra of AEDANS-60-Tn on reconstituted thin filaments in the presence (curves 2 and 5) and absence (curves 1 and 4) of the acceptor (DABMI bound to F-actin). These spectra were measured under the same solvent conditions as in Figure 1 but with DABMI bound to Cys-374 as the acceptor instead of FLC bound to Gln-41 of actin.

FRET between DAB-F-actin and AEDANS-60-Tn or AEDANS-250-Tn showed a similar Ca^{2+}-induced change in the transfer efficiency to that observed with FLC-F-actin. The donor fluorescence was more strongly quenched in the absence than in the presence of Ca^{2+}, indicating that Cys-60 and Cys-250 on TnT move closer to Cys-374 on F-actin in the absence of Ca^{2+}.

To obtain more quantitative data on the transfer effi-

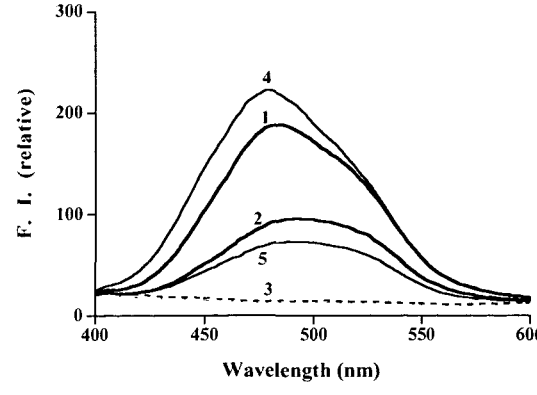

Fig. 2. **Fluorescence spectra of AEDANS bound to Cys-60 of TnT on reconstituted thin filaments in the presence and absence of an acceptor (DABMI bound to Cys-374 of actin).** (1) F-actin/Tm/AEDANS-Tn/$+Ca^{2+}$, (2) DAB-F-actin/Tm/AEDANS-Tn/$+Ca^{2+}$, (3) DAB-F-actin/Tm/Tn/$\pm Ca^{2+}$, (4) F-actin/Tm/AEDANS-Tn/$-Ca^{2+}$, (5) DAB-F-actin/Tm/AEDANS-Tn/$-Ca^{2+}$. Spectra were measured under the same conditions as in Fig. 1.

ciency, the ratio of donor fluorescence quenching was measured by titrating AEDANS-Tn/Tm with FLC-F-actin in the presence (buffer F + 50 μM $CaCl_2$) and absence of Ca^{2+} (buffer F + 1 mM EGTA) at 20°C (Fig. 3). The fluorescence intensity was measured at 460 nm, where the acceptor- fluorescence from FLC makes no contribution, as seen in Fig. 1. To correct for the fluorescence intensity change of AEDANS-Tn upon binding to an F-actin filament, the same amount of non-labeled F-actin was added to the AEDANS-Tn/Tm as reference, and the ratio of these fluorescence intensities was taken as the relative fluorescence intensity. The apparent decrease of the fluorescence intensity due to inner filter effects arising from the absorbance of FLC-F-actin was corrected according to Eq. 5. The relative fluorescence intensity decreased gradually in the actin/Tn molar ratio range up to 7 and became almost constant in the range over 7 on the reconstituted thin filament. From the saturation points, the apparent energy transfer efficiencies were calculated to be 0.54 ± 0.02 for the $+Ca^{2+}$ state and 0.67 ± 0.01 for the $-Ca^{2+}$ state in the case of AEDANS-60-Tn, and 0.81 ± 0.02 for the $+Ca^{2+}$ state and 0.93 ± 0.01 for the $-Ca^{2+}$ state in the case of AEDANS-250-Tn. These transfer efficiencies correspond to distances of 42.1 ± 0.6 Å for the $+Ca^{2+}$ state and 39.5 ± 0.3 Å for the $-Ca^{2+}$ state in the case of AEDANS-60-Tn, and 35.8 ± 0.8 Å for the $+Ca^{2+}$ state and 30.0 ± 0.8 Å for the $-Ca^{2+}$ state in the case of AEDANS-250-Tn.

AEDANS-60-Tn/Tm and AEDANS-250-Tn/Tm were also titrated with DAB-F-actin in the same way as FLC-F-actin except for measuring fluorescence intensities at 490 nm instead of 460 nm (Fig. 4). The energy transfer efficiencies obtained were 0.61 ± 0.02 and 0.78 ± 0.01 in the case of AEDANS-60-Tn for the $+Ca^{2+}$ and $-Ca^{2+}$ states, respectively, and 0.59 ± 0.01 and 0.85 ± 0.01 in the case of AEDANS-250-Tn for the $+Ca^{2+}$ and $-Ca^{2+}$ states, respectively. These transfer efficiencies correspond to distances of 34.4 ± 0.2 Å and 30.8 ± 0.3 Å for the $+Ca^{2+}$ and $-Ca^{2+}$ state, respectively in the case of AEDANS-60-Tn, and 36.6 ± 0.2 Å and 29.6 ± 0.4 Å for the $+Ca^{2+}$ and $-Ca^{2+}$ state, respectively in the case of AEDANS-250-Tn.

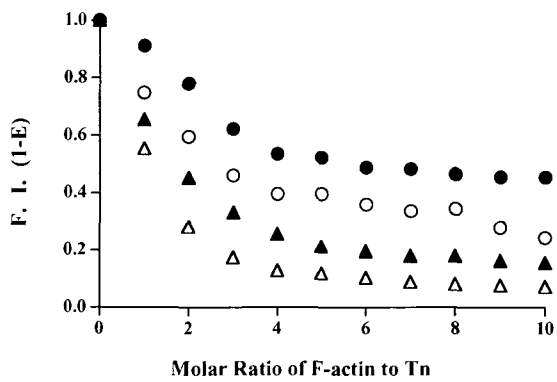

Fig. 3. **Relative fluorescence intensities of AEDANS bound to Cys-60 (● for $+Ca^{2+}$ and ○ for $-Ca^{2+}$ state) and Cys-250 (▲ for $+Ca^{2+}$ and △ for $-Ca^{2+}$ state) of TnT in the Tn-Tm complex vs. molar ratio of FLC-F-actin.** Values were obtained in buffer F and 50 μM $CaCl_2$ ($+Ca^2$) or 1mM EGTA ($-Ca^{2+}$) at 20°C, after correction for the inner filter effects according to Eq. 5. The concentrations of AEDANS-Tn and Tm were 0.042 and 0.044 mg/ml, respectively. Excitation was at 340 nm and emission was measured at 460 nm.

The transfer efficiencies and distances are summarized in Table I. Compared with Cys-60 of TnT, Cys-250 of TnT is located much closer to Gln-41 of F-actin regardless of whether Ca^{2+} is present or not. Cys-250 of TnT moves more than Cys-60 in response to the binding of Ca^{2+} to Tn. FRET showed that Cys-133 of TnI, which is located near the inhibitory region, moved away about 10 Å from F-actin upon binding of Ca^{2+} to TnC (*16–19*). On the other hand, the C-terminal region of TnT interacts with the globular region of Tn (TnI and C) (*32*). In accordance with this, FRET demonstrated that the C-terminal region of TnT moves away together with the inhibitory region of TnI upon binding of Ca^{2+} to TnC. The present FRET measurements showed that not only the C-terminal region but also the N-terminal region of TnT moved significantly upon binding of Ca^{2+} to TnC.

Effects of S1 Binding on FRET between AEDANS-60-Tn or AEDANS-250-Tn and FLC or DAB-F-Actin on Reconstituted Thin Filamensts—Fluorescence spectra of AEDANS bound to Cys-60 or Cys-250 of TnT on reconstituted thin filaments were measured in the presence of S1, using DABMI bound to actin as the energy acceptor. The solvent conditions were buffer F + 50 μM $CaCl_2$ for the $+Ca^{2+}$ state and buffer F + 1 mM EGTA for the $-Ca^{2+}$ state at 20°C. In the absence of the acceptor, the donor fluorescence intensities were decreased by the addition of S1 (1/3 mole ratio to

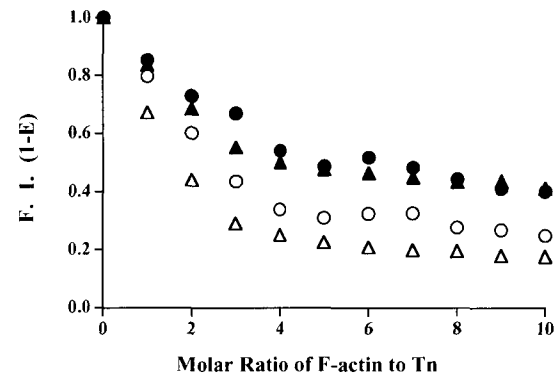

Fig. 4. **Relative fluorescence intensities of AEDANS bound to Cys-60 (● for $+Ca^{2+}$ and ○ for $-Ca^{2+}$ state) and Cys-250 (▲ for $+Ca^{2+}$ and △ for $-Ca^{2+}$ state) of TnT in the Tn-Tm complex vs. molar ratio of DAB-F-actin.** Values were obtained in buffer F and 50 μM $CaCl_2$ ($+Ca^2$) or 1 mM EGTA ($-Ca^{2+}$) at 20°C, after correction of the inner filter effects according to Eq. 5. The concentrations of AEDANS-Tn and Tm were 0.042 and 0.044 mg/ml, respectively. Excitation was at 340 nm and emission was measured at 490 nm.

TABLE I. **Distances between probes attached to Tn and actin in reconstituted thin filaments in the presence and absence of Ca^{2+} ions.**

Donor site (Tn)	Acceptor site (F-actin)	Ca^{2+}	R_0 (2/3) (Å)	Efficiency	R(2/3) (Å)
TnT60	Gln-41	+	43.3	0.54 ± 0.02	42.1 ± 0.6
		−	44.3	0.67 ± 0.01	39.5 ± 0.3
	Cys-374	+	37.1	0.61 ± 0.02	34.4 ± 0.2
		−	37.9	0.78 ± 0.01	30.8 ± 0.3
TnT250	Gln-41	+	45.6	0.81 ± 0.02	35.8 ± 0.8
		−	46.3	0.93 ± 0.01	30.0 ± 0.8
	Cys-374	+	38.9	0.59 ± 0.01	36.6 ± 0.2
		−	39.4	0.85 ± 0.01	29.6 ± 0.4

actin) for the $-Ca^{2+}$ state. On the other hand, the intensities did not change appreciably for the $+Ca^{2+}$ state. In the presence of the acceptor, however, the addition of S1 increased the donor fluorescence intensities significantly for both $+Ca^{2+}$ and $-Ca^{2+}$ states. The addition of ATP (1 mM) reversed the changes in FRET induced by rigor S1 binding, and after complete hydrolysis of ATP the changes in FRET were again observed.

To obtain quantitative data for the S1-induced conformational change, changes in the FRET efficiency of AEDANS-60-Tn or AEDANS-250-Tn and Tm/DAB-F-actin were measured after the addition of various amounts of S1 in the presence and absence of Ca^{2+} (Fig. 5). To correct for the dilution effects and fluorescence changes of AEDANS-Tn induced by the addition of S1, the same amounts of S1 were added to the AEDANS-Tn/Tm/F-actin as a reference, and the ratios of these fluorescence intensities at 490 nm were taken as the relative fluorescence intensity. To eliminate the scattering effects of S1, non-fluorescent samples of Tn/Tm/DAB-F-actin were prepared under the same solvent conditions as FRET samples, and the same amounts of S1 were added. Then the scattered light of these non-fluorescent samples was measured under the same experimental conditions as the FRET samples, and their intensities were subtracted from the fluorescence intensities of FRET samples. The extent of the S1-induced conformational change increased as the molar ratio of S1 to actin increased, and was saturated before a molar ratio of 1.0 in the presence of Ca^{2+}. Assuming that all thin filaments are in the S1-induced state at the molar ratio of 1, the distances between Cys-60 or Cys-250 of TnT and Cys-374 of F-actin on reconstituted thin filaments were 38.9 ± 0.8 and 41.0 ± 0.7 Å, respectively in the S1-induced state. S1-rigor binding increased the distance between Cys-60 of TnT and Cys-374 of F-actin by ~5 Å, and the distance between Cys-250 of TnT by ~4 Å in the presence of Ca^{2+}. The extent of S1-induced conformational change also increased with increase in the molar ratio of S1 to actin in the absence of Ca^{2+}. The relative fluorescence intensities $(1 - E)$ at the molar ratio of 1 increased to the same level as those in the presence of Ca^{2+}.

The effects of S1 binding on FRET between AEDANS-60- or AEDANS-250-Tn and FLC-F-actin were also measured under the same experimental conditions as DAB-F-actin except that fluorescence intensity was measused at 460 nm instead of 490 nm (Fig. 6). The extent of the S1-induced conformational change increased as the molar ratio of S1 increased in both the presence and absence of Ca^{2+} in the same way as in the case of DAB-F-actin. S1-rigor binding increased the distance between Cys-60 of TnT and Gln-41 of F-actin further by ~4 Å and the distance between Cys-

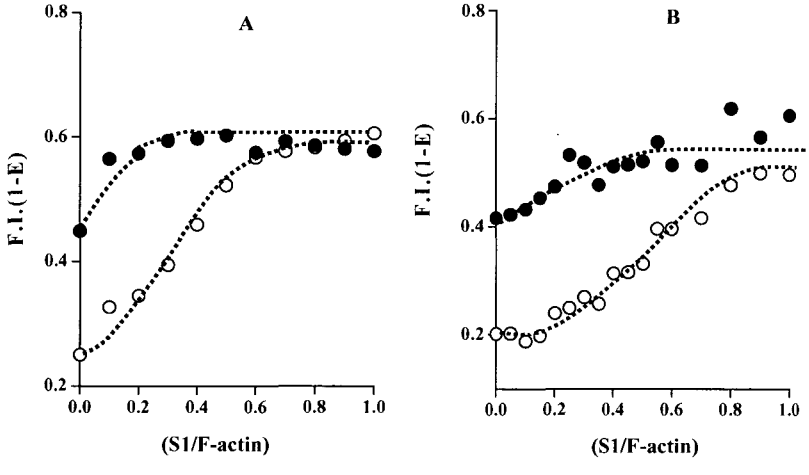

Fig. 5. **Relative fluorescence intensities $(1 - E)$ of AEDANS bound to Cys-60 (A) and Cys-250 (B) of TnT in the reconstituted thin filaments *vs.* molar ratios of S1 to actin. Resonance energy acceptor was DABMI, which attached to Cys-374 of actin.** Values were obtained in buffer F and 50 μM $CaCl_2$ for the $+Ca^{2+}$ state (●) or 1 mM EGTA for the $-Ca^{2+}$ state (○) at 20°C. A small volume of a concentrated S1 solution was added stepwise. To correct for dilution effects, the sample containing of non acceptor-labeled F-actin instead of DAB-F-actin was used as a reference, and the ratio of fluorescence intensities was taken. The concentrations of F-actin, Tm, and Tn were 0.23, 0.044, and 0.042 mg/ml, respectively. Fluorescence measurements were carried out after hydrolysis of contaminant ATP (less than 10 μM). Excitation was at 340 nm and emission was measured at 490 nm.

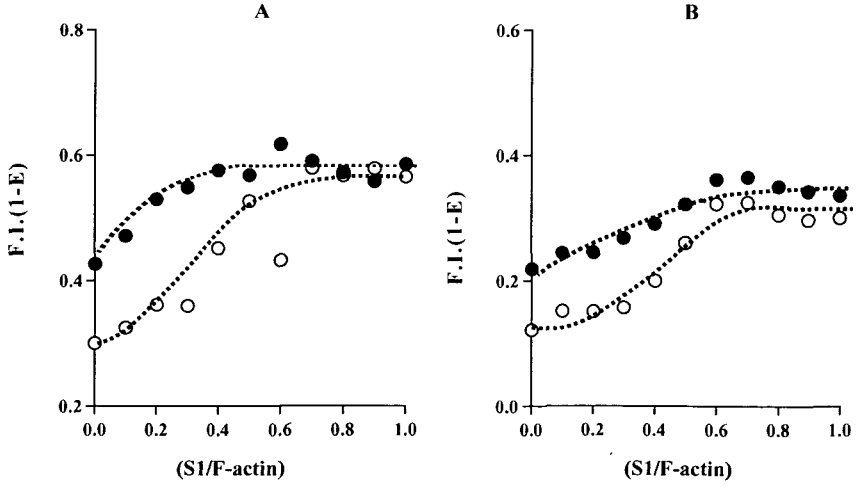

Fig. 6. **Relative fluorescence intensities $(1 - E)$ of AEDANS bound to Cys-60 (A) and Cys-250 (B) of TnT in the reconstituted thin filaments *vs.* molar ratios of S1 to actin. Resonance energy acceptor was FLC, which attached to Gln-41 of actin.** Values were obtained in buffer F and 50 μM $CaCl_2$ for the $+Ca^{2+}$ state (●) or 1 mM EGTA for the $-Ca^{2+}$ state (○) at 20°C. The data were corrected by the same calculation as in Fig. 5. The concentrations of F-actin, Tm, and Tn were 0.23, 0.044, and 0.042 mg/ml, respectively. Fluorescence measurements were carried out after hydrolysis of contaminant ATP (less than 10 μM). Excitation was at 340 nm and emission was measured at 460 nm.

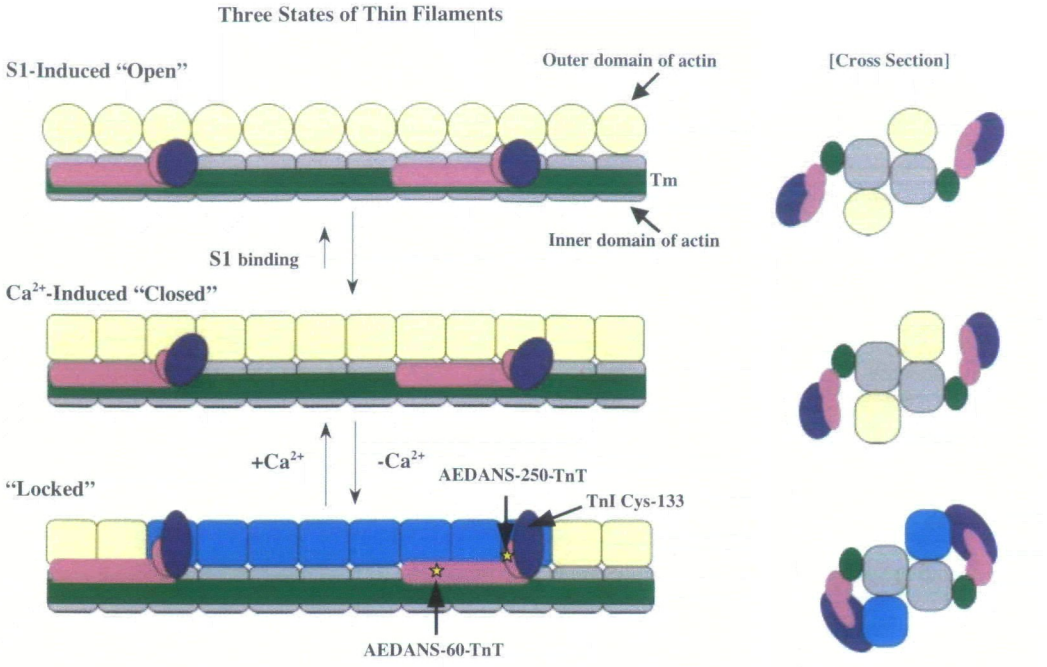

Fig. 7. **A schematic model of Tn and Tm along the long-pitch helix of an actin filament in three states of thin filaments (left side) and a cross section of the thin filament (right side). One actin molecule is illustrated with two frames that represent its outer and inner domains.** One Tm covers the inner domains of seven actin monomers along the long-pitch helix. In the absence of Ca^{2+}, thin filaments are in the locked state. N- and C-terminal domains of TnT turn over to the outer domain of actin, and C-terminal domain is closer to the outer domain of actin than N-terminal domain. Two neighboring TnIs along Tm cross-link the outer domains of two actin monomers and lock eight actin monomers in the off-state in combination with Tm. Upon Ca^{2+} binding to TnC, the latchkey of TnI is released, and the thin filament shifts to closed state (or Ca^{2+}-induced state). N- and C-terminal domains of TnT also move toward the inner domain of actin. In this state, the key is unlocked but the door is still closed. Myosin binding induces a conformational change in actin monomers, and both TnI and TnT detach further away from actin. Now the door is open and the thin filament is in the open state. Several strongly bound S1 (rigor complex or NEM-treated S1) molecules on a unit length of an actin filament distort the filament structure, which forces N- and C-terminal domain of TnT and the latchkey of TnI to detach even in the absence of Ca^{2+}. Then, the thin filament is transformed to the open state even in the absence of Ca^{2+}. Each color in the cross section (right side) corresponds to schematic model of thin filament (left side).

250 of TnT and Gln-41 of F-actin by ~5 Å in the presence of Ca^{2+}. In the absence of Ca^{2+}, the relative fluorescence intensities $(1 - E)$ at the molar ratio of 1 increased to the same level as those in the presence of Ca^{2+}. It should be emphasized here that curves of S1-induced change in Fig. 5 and 6 were hyperbolic for AEDANS-60-Tn and nearly hyperbolic for AEDANS-250-Tn in the presence of Ca^{2+}, but distinctly sigmoidal in the absence of Ca^{2+}.

DISCUSSION

In calculating the distances between probes, we used the value of 2/3 for the orientation factor, which corresponds to the case where both donor and acceptor molecules rotate freely and rapidly. The limiting anisotropy values of probes bound to proteins are usually much lower than the fundamental anisotropy values, suggesting that the probes showed limited very rapid motion in sub-nanosecond time-scale. However, the time-resolved anisotropy decay measurements showed that the probes attached to F-actin do not rotate freely and that the motion of the probes is in the range from several hundred nanoseconds to several milliseconds (*33–35*). Although the motions of probes are slow on the nanosecond time-scale, segmental flexibility of proteins can lead to randomized directions of the transition moments of probes on a long time-scale. Therefore, the actual value for the orientation factor is probably very close to 2/3. Indeed, we have pointed out that reasonable agreement was obtained between intra- and inter-molecular distances in G-actin and F-actin determined by FRET assuming $\kappa^2 = 2/3$ and the distances determined from X-ray diffraction data (*15*). Although internal motions of probes attached to F-actin are changed by Ca^{2+}- or S1-binding in the range from several hundred nanoseconds to several milliseconds (*33–35*), mutual directions of donor and acceptor molecules on thin filaments are randomized on a long time-scale as in an equilibrium state. Therefore, the changes in transfer efficiency in the present FRET measurements could be attributed mainly to changes in distances between probes.

Using the steric blocking model as a working hypothesis, many structural works have been performed. X-ray diffraction and 3D-EM data have been interpreted to indicate Tm movement in response to functional states of the thin filament (*10, 11*). On the other hand, FRET measurements did not detect any significant movement of Tm on thin filaments (*16, 21–24*). Squire and Morris (*36*) suggested that movement of the whole troponin complex, without movement of tropomyosin itself, could explain the changes in intensity of the X-ray diffraction pattern of activated muscle and the Ca^{2+}-induced strand movement observed in 3D-EM. Instead of Tm movement, FRET measurements showed the Ca^{2+}-induced movement of TnI (*16–21*). On stopped-flow fluorometry, the time rate of this movement was first enough to allow this TnI movement on actin filaments to be directly involved in the activation of muscle contraction (*18*). Recent kinetic studies proposed a three-state model of thin filaments: a blocked state, in which muscle is relaxed; a closed state, which is induced by Ca^{2+} binding to Tn; and an open state, which is induced by

strong S1 binding (*7, 8*). These states have subsequently been described in terms of the position of Tm on the actin filament, supporting the steric blocking model (*10, 11*). Although no significant Tm movement was detected, FRET measurements showed three positions of TnI corresponding to three states of a thin filament (*20, 21*). Furthermore, FRET (*21*) demonstrated that this S1-induced TnI movement is impaired on a functionally deficient mutant tropomyosin, D234Tm, which lacks internal actin-binding pseudo-repeats 2, 3, and 4 (*37*). Since D234Tm always inhibits the acto-S1 ATPase activity whether Ca^{2+} is present or not, S1-induced TnI movement corresponds well to a functional state of the thin filament.

Although significant mass movement of TnI was observed during on-off switching in regulation, mass movement of other components of Tn has not been observed. In this study, we generated two mutant TnT 25-kDa fragments, TnT25k (E60C) and TnT25k (S250C), to investigate whether TnT moves in response to the three states of thin filaments as observed in TnI. TnT extends along the C-terminal third of Tm, and the N-terminus of TnT binds to the head-to-tail overlap region of two adjacent Tm molecules (*32*). TnI and TnC bind to the C-terminal region of TnT and form a globular portion of Tn. The globular portion of the troponin complex is located near residues 150-180 on Tm (*38*). Therefore, the two labeling sites were expected to be far apart from each other on TnT and also along the thin filament. Both chymotryptic fragments of TnT, TnT1 and TnT2, bind to Tm, but in a Ca^{2+}-independent and Ca^{2+}-dependent manner, respectively. The binding region within TnT1 is in the α-helical region of residues 71–150, which can thus form a stable triple-stranded binding structure with the coiled-coil Tm (*39*). Therefore, the residue 60 (E60C) seems to be located near this Tm-binding site. In fragment TnT2, the main binding region to Tm is located in the small C-terminal region of 17 residues (*3*). Residue 250 is localized in the region that is critical for the Ca^{2+}-sensitizing activity of TnT. The FRET between Cys-250 of TnT and Gln-41 of actin in the absence of Ca^{2+} showed 93% transfer efficiency, the highest value ever obtained in FRET measurements between troponin components or tropomyosin and actin. On the other hand, the distance from Cys-60 of TnT to Gln-41 of actin is larger than that from Cys-250 of TnT but smaller than that from Cys-190 of Tm to the same residue. Tm is located on the inner domain of the actin helix (*40*). Cys-60 of TnT is located close to the Tm binding site, and Cys-250 of TnT in combination with the globular parts of troponin TnC and TnI seems to project towards the outer domain of actin.

The present FRET measurements showed that the distances between Cys-60 or Cys-250 of TnT and Gln-41 or Cys-374 of actin on thin filaments increased upon Ca^{2+} and S1 binding. This indicates either that TnT detached further away from actin, or that the outer domain of actin moved further away from TnT, since Gln-41 and Cys-374 are located on the outer domain of actin. If the latter is the case, the distance between probes attached to Tm and actin (Gln-41 and Cys-374) should also be changed upon Ca^{2+} and S1 binding, since Tm is located on the inner domain of actin (*40*) and TnT binds to Tm. But the distance between probes on Tm and actin did not appreciably change upon Ca^{2+} and S1 binding (*21*). Therefore, it seems more likely that TnT with TnI moves away from the outer domain of actin upon Ca^{2+} and S1 binding.

FRET measurements demonstrated a large Ca^{2+}-induced movement of the C-terminal region of TnT. The distance change was ~6 Å from Gln-41 and ~7 Å from Cys-374 of actin, which was smaller than the distance change observed in Cys-133 of TnI but nearly comparable with that in the N-terminus of TnI (*19*). Furthermore, the N-terminal region of TnT also showed a substantial amount of Ca^{2+}-induced movement (3-4 Å). The present FRET measurements suggest that upon binding of Ca^{2+} to TnC, significant amounts of mass of the troponin molecule shift from the vicinity of the outer domain to the vicinity of the inner domain of actin. This mass movement of the troponin molecule could explain the changes in intensity of the X-ray diffraction pattern of activated muscle and the Ca^{2+}-induced strand movement observed in 3D-EM, without assuming any significant movement of Tm (*36*).

FRET measurements demonstrated the S1-induced movement of TnI, but no significant movement of Tm. Therefore, the name "locked state" was used instead of "blocked state" for one of the three states of thin filaments in our model (*21*). During the transition from the locked to the closed state, Cys-133 of TnI moves away the outer domain of actin on the thin filament by ~10 Å, and further away by ~7 Å during the transition from the closed to the open state. Even in the absence of Ca^{2+}, the transition from the locked to the open state occurs when sufficient amounts of S1 bind to thin filaments in the absence of ATP. However, the addition of ATP reversed the S1-induced transition both in the presence and absence of Ca^{2+}. This means that the population of strongly bound S1 is small during the Mg-ATPase cycle, and only the strongly bound S1 induces the transition from the closed to the open state. These results explain the well-known experimental evidence that, even in the absence of Ca^{2+}, the thin filament-activated Mg-ATPase rate of unmodified S1 increases on the addition of NEM-S1, which binds tightly to actin even in the presence of ATP (*41*). On the other hand, the transition curve in the absence of Ca^{2+} was sigmoidal vs. molar ratio of S1 to actin, while the transition curve in the presence of Ca^{2+} was hyperbolic. This means that, in the presence of Ca^{2+}, a single strongly bound S1 molecule per unit length of actin filament can induce the transition to the open state, while in its absence, several strongly bound S1 molecules are required per unit length of actin filament. However, the population of strongly bound S1 during the ATPase cycle is very low, and consequently the probability that several strongly bound S1 molecules stay simultaneously on a unit length of actin filament is extremely low. The results explain why the ATPase rate of unmodified S1 is activated in the presence but not in the absence of Ca^{2+}.

The present FRET measurements demonstrated that not only TnI but also TnT changes its position on the thin filament in response to three states of the thin filament. Plots of the extent of the S1-induced conformational change vs. added S1 (Figs. 5 and 6) showed that the curve in the presence of Ca^{2+} is hyperbolic for AEDANS-60-Tn or nearly hyperbolic for AEDANS-250-Tn, whereas the curve in the absence of Ca^{2+} is sigmoidal for both AEDANS-60- and AEDANS-250-Tn. The results support the notion of three states of thin filaments and also the importance of Tn movement for the regulation of the skeletal muscle thin filament. In comparison with the C-terminal region (Cys-250)

of TnT, the S1-induced movement of N-terminal region (Cys-60) saturated at a smaller molar ratio of added S1 to actin. The results suggest that the TnT subunit moved on the thin filament by strong S1 binding not as a solid rod but as a flexible rod.

In the previous paper (*21*), we presented a schematic model of Tn and Tm along the long-pitch helix of an actin filament in three states of thin filaments observed from our FRET measurements. In that model, the shift of TnI was indicated corresponding to three states of thin filaments, but the shift of TnT was not considered. A new model including a movement of TnT is illustrated in Fig. 7. Except for TnT movement, the present model is essentially the same as the previous one. In that model (*21, 24, 42*), Tn acts as a Ca^{2+}-sensing latch, and in combination with Tm, regulates the flexibility of thin filaments that is important for smooth interaction between actin and myosin during ATPase cycle. When the two neighboring TnIs along the long-pitch helix cross-link two actin monomers, they may cause considerable distortion of the actin helix and/or significant inhibition of internal motion of the outer domains of eight actin monomers, which are located between two neighboring cross-links along the long-pitch helix. Thus, local movement of the troponin complex, in combination with Tm, can cause complete inhibition along the whole actin filament, instead of steric blocking by Tm.

We wish to thank the Food Research and Development Laboratories of Ajinomoto Co. for the generous gift of microbial transglutaminase, and Prof. I. Muramatsu of Fukui Medical University for kindly providing the rabbit hearts.

REFERENCES

1. Ebashi, S., Endo, M., and Ohtsuki, I. (1969) Control of muscle contraction. *Q. Rev. Biophys.* **2**, 351–384
2. Ohtsuki, I. (1979) Molecular arrangement of troponin T in the thin filament. *J. Biochem.* **86**, 491–497
3. Onoyama, Y. and Ohtsuki, I. (1986) Effect of chymotryptic troponin T subfragments on the calcium ion-sensitivity of ATPase and superprecipitation of actomyosin. *J. Biochem.* **100**, 517–519
4. Ohtsuki, I., Shiraishi, F., Suenaga, N., Miyata, I., and Tanokura, M. (1984) A 26K fragment of troponin T from rabbit skeletal muscle. *J. Biochem.* **95**, 1337–1342
5. Fujita, S., Maeda, K., and Maéda, Y. (1992) Expression in *Escherichia coli* and a functional study o f a b-troponin T 25 kDa fragment of rabbit skeletal muscle. *J. Biochem.* **112**, 306–308
6. Gordon, A.M., Homsher, E., and Regnier, M. (2000) Regulation of contraction in striated muscle. *Physiol. Rev.* **80**, 853–924
7. Mckillop, D.F. and Geeves, M.A. (1993) Regulation of the interaction between actin and myosin subfragment 1: evidence for three states of the thin filament. *Biophys. J.* **65**, 693–701
8. Geeves, M.A. and Lehrer, S.S. (1994) Dynamics of the muscle thin filament regulatory switch: the size of the cooperative unit. *Biophys. J.* **67**, 273–282
9. Lehrer, S.S. and Geeves, M.A. (1998) The muscle thin filament as a classical cooperative/allosteric regulatory system. *J. Mol. Biol.* **277**, 1081–1089
10. Holmes, K.C. (1995) The actomyosin interaction and its control by tropomyosin. *Biophys. J.* **68** (suppl.), 2–7
11. Vibert, P., Craig, R., and Lehman, W. (1997) Steric-model for activation of muscle thin filamenents. *J. Mol. Biol.* **266**, 8–14
12. Lehman, W., Rosol, M., Tobacman, L. S., and Craig, R. (2001) Troponin organization on relaxed and activated thin filaments revealed by electron microscopy and three-dimensional reconstruction. *J. Mol. Biol.* **307**, 739–744
13. Narita, A., Yasunaga, T., Ishikawa, T., Mayanagi, K., and Wakabayashi, T. (2001) Ca^{2+}-induced switching of troponin and tropomyosin on actin filaments as revealed by electron cryo-microscopy. *J. Mol. Biol.* **308**, 241–261
14. dos Remedios, C.G., Miki, M., and Barden, J.A. (1987) Fluorescence resonance energy transfer measurements of distances in actin and myosin. A critical evaluation. *J. Muscle Res. Cell Motil.* **8**, 97–117
15. Miki, M., O'Donoghue, S.I., and dos Remedios, C.G. (1992) Structure of actin observed by fluorescence resonance energy transfer spectroscopy. *J. Muscle Res. Cell Motil.* **13**, 132–145
16. Miki, M. (1990) Resonance energy transfer between points in a reconstituted skeletal muscle thin filament : A conformational change of the thin filament in response to a change in Ca^{2+} concentration. *Eur. J. Biochem.* **187**, 155–162
17. Tao, T., Gong, B.J., and Leavis, P.C. (1990) Calcium-induced movement of troponin-I relative to actin in skeletal musde thin filaments. *Science* **247**, 1339–1341
18. Miki, M. and Iio, T. (1993) Kinetics of structural changes of reconstituted skeletal muscle thin filaments observed by fluorescence resonance energy transfer. *J. Biol. Chem.* **268**, 7101–7106
19. Miki, M., Kobayashi, T., Kimura, H., Hagiwara, A., Hai, H., and Maéda, Y. (1998) Ca^{2+}-induced distance change between points on actin and troponin in skeletal muscle thin filaments estimated by fluorescence resonance energy transfer spectroscopy. *J. Biochem.* **123**, 324–331
20. Kobayashi, T., Kobayashi, M., and Collins, J.H. (2001) Ca^{2+}-dependent, myosin subfragment 1-induced proximity changes between actin and the inhibitory region of troponin I. *Biochim. Biophys. Acta* **1549**, 148–154
21. Hai, H., Sano, K., Maeda, K., Maéda Y. and Miki, M. (2002) Ca^{2+}-induced conformational change of reconstituted skeletal muscle thin filaments with an internal deletion mutant D234-tropomyosin observed by fluorescence energy transfer spectroscopy: structural evidence for three states of thin filament. *J. Biochem.* **131**, 407–418
22. Miki, M. and Mihashi, K. (1979) Conformational changes of reconstituted thin filament under the influence of Ca^{2+} ion-Fluorescence energy transfer and anisotropy decay measurements (in Japanese). *Seibutsu-Butsuri* **19**, 135-140
23. Tao, T., Lamkin, M., and Lehrer, S.S. (1983) Excitation energy transfer studies of the proximity between tropomyosin and actin in reconstituted skeletal muscle thin filaments. *Biochemistry* **22**, 3059–3066
24. Miki, M., Miura, T., Sano, K., Kimura, H., Kondo, H., Ishida, H., and Maéda, Y. (1998) Fluorescence resonance energy transfer between points on tropomyosin and actin in skeletal muscle thin filaments: Does tropomyosin move? *J. Biochem.* **123**, 1104–1111
25. Fujita, S., Maeda, K., and Maéda, Y. (1991) Complete coding sequences of cDNAs of four variants of rabbit skeletal musde troponin T. *J. Muscle Res. Cell Motil.* **12**, 560–565
26. Akiyama, Y. and Itoh, K. (1990) SECY protein, a membrane-embedded secretion factor of E. coli, is cleaved by the OMPT protease in vitro. *Biochem. Biophys. Res. Commun.* **167**, 711–715
27. Lamkin, M., Tao, T., and Lehrer, S.S. (1983) Tropomyosin-troponin and tropomyosin-actin interactions: a fluorescence quenching study. *Biochemistry* **22**, 3053–3058
28. Lorand, L., Parameswaran, K.N., Velasco, P.T., Hsu, L.K.-H., and Siefring, G.E., Jr. (1983) New colored and fluorescent amine substrates for activated fibrin stabilizing factor (Factor XIIIa) and for transglutaminase. *Anal. Biochem.* **131**, 419–425
29. Hudson, E.N. and Weber, G. (1973) Synthesis and characterization of two fluorescent sulfhydryl reagents. *Biochemistry* **12**, 4154–4161
30. Scott, T.G., Spencer, R.D., Leonard, N.G., and Weber, G. (1970) Emission properties of NADH. Studies of fluorescence lifetimes and quantum efficiencies of NADH, AcPyADH, and simplified synthetic models. *J. Am. Chem. Soc.* **92**, 687–695
31. Tausky, H.H. and Shorr, E. (1953) A microcolorimetric method for the determination of inorganic phosphorus. *J. Biol. Chem.*

202, 675–685
32. Ohtsuki, I., Maruyama, K., and Ebashi, S. (1986) regulatory and cytoskeletal proteins of vertebrate skeletal muscle. *Adv Protein Chem.* **38**, 1–67
33. Miki, M., Wahl, Ph., and Auchet, J.-C. (1982) Fluorescence anisotropy of labeled F-actin: Influence of divalent cations on the interaction between F-actin and myosin heads. *Biochemistry* **21**, 3661–3665
34. Thomas, D.D., Seidel, J.C., and Gergely, J. (1979) Rotational dynamics of spin-labeled F-actin in the sub-millisecond time range. *J. Mol. Biol.* **132**, 257–273
35. Yoshimura, H., Nishio, T., Mihashi, K., Kinosita, K., and Ikegami, A. (1984) Torsional motion of eosin-labeled F-actin as detected in the time-resolved anisotropy decay of the probe in the sub-millisecond time range. *J. Mol. Biol.* **179**, 453–467
36. Squire, J.M. and Morris, E.P. (1998) A new look at thin filament regulation in vertebrate skeletal muscle. *FASEB J.* **12**, 761–771
37. Landis, C.A., Bobkova, A., Homsher, E., and Tobacman, L.S. (1997) The active state of the thin filament is destabilized by an internal deletion in tropomyosin. *J. Biol. Chem.* **272**, 14051–14056
38. White, S.P., Cohen, C., and Phillips Jr, G.N. (1987) Structure of co-crystals of tropomyosin and troponin. *Nature* **325**, 826–828
39. Nagano, K., Miyamoto, S., Matsumura, M., and Ohtsuki, I. (1981) Possible formation of a triple-stranded coiled-coil region in tropomyosin-troponin T binding complex. *J. Mol. Biol.* **141**, 217–222.
40. Saeki, K., Sutoh, K., and Wakabayashi, T. (1996) Tropomyosin binding site(s) on the *Dictyostelium* actin surface as identified by site-directed mutagenesis. *Biochemistry* **35**, 14465–14472.
41. Pemrick, S. and Weber, A. (1976) Mechanism of inhibition of relaxation by N-ethylmaleimide treatment of myosin. *Biochemistry* **15**, 5193–5198
42. Miki, M. (2002) Structural changes between regulatory proteins and actin: A regulation model by tropomyosin-troponin based on FRET measurements in *Molecular Interactions of Actin*, Vol. 2 (Thomas, D.D. and dos Remedios, C.G., eds.) pp. 191–203, Springer Verlag, Heidelberg